Exploration of BAY 11-7082 as a novel antibiotic

Victoria E. Coles[a,b], Patrick Darveau[c], Xiong Zhang[a], Hanjeong Harvey[a,b], Brandyn D. Henriksbo[b], Angela Yang[a,b], Jonathan D. Schertzer[b], Jakob Magolan[a,b,c], and Lori L. Burrows[a,b] *

[a]*Department of Biochemistry and Biomedical Sciences, McMaster University, 1280 Main Street W. Hamilton, Ontario, L8S 4K1, Canada*

[b]*Michael G. DeGroote Institute for Infectious Disease Research, McMaster University, 1280 Main Street W. Hamilton, Ontario, L8S 4K1, Canada*

[c]*Department of Chemistry and Chemical Biology, McMaster University, 1280 Main Street W. Hamilton, Ontario, L8S 4L8, Canada*

*Email: lori.burrows@mcmaster.ca

Abstract

Exposure of the Gram-negative pathogen *Pseudomonas aeruginosa* to sub-inhibitory concentrations of antibiotics increases formation of biofilms. We exploited this phenotype to identify molecules with potential antimicrobial activity in a biofilm-based high-throughput screen. The anti-inflammatory compound BAY 11-7082 induced dose-dependent biofilm stimulation, indicative of antibacterial activity. We confirmed that BAY 11-7082 inhibits growth of *P. aeruginosa* and other priority pathogens, including methicillin-resistant *Staphylococcus aureus* (MRSA). We synthesized 27 structural analogues, including a series based on the related scaffold 3-(phenylsulfonyl)-2-pyrazinecarbonitrile (PSPC), 10 of which displayed increased anti-*Staphylococcal* activity. Because the parent molecule inhibits the NLR Family Pyrin Domain Containing 3 (NLRP3) inflammasome, we measured the ability of select analogues to reduce IL-1β production in mammalian macrophages, identifying minor differences in the structure-activity relationship for the anti-inflammatory and antibacterial properties of this scaffold. Although we could evolve stably resistant MRSA mutants with cross resistance to BAY 11-7082 and PSPC, their lack of shared mutations suggested that the two molecules could have multiple targets. Finally, we showed that BAY 11-7082 and its analogues potentiate the activity of penicillin G against MRSA, suggesting that this scaffold may serve as an interesting starting point for the development of antibiotic adjuvants.

Keywords:

Methicillin resistant *Staphylococcus aureus*; biofilm; antibiotics; drug discovery

Introduction

The overuse and misuse of antibiotics has selected for resistant bacteria, increasing the prevalence of drug-resistant infections. As resistance renders standard treatment options less effective, there is a need for the development of novel pharmaceuticals to treat those infections, particularly those caused by the ESKAPE (*Enterococcus faecium*, *Staphylococcus aureus*, *Klebsiella pneumoniae*, *Acinetobacter baumannii*, *Pseudomonas aeruginosa*, and *Enterobacter* species) pathogens.[1,2] Despite this urgent need, approval of new antimicrobials by the Food and Drug Administration (FDA) has decreased in recent decades, with only nine new antibiotics approved between 1998-2002.[3] The rate of approval increased slightly within the last ten years, with eight new antibiotics approved between 2010-2015; however, of these, only three are active against ESKAPE pathogens and only one has a novel mechanism of action, with the rest belonging to established antibiotic classes.[4]

Development of novel antimicrobials with potent activity against the ESKAPE pathogens – including methicillin-resistant *S. aureus* (MRSA) – is crucial. Since strains of MRSA are extensively β-lactam resistant, treatment options are scarce. They include vancomycin, daptomycin, linezolid, tetracyclines, and rifampin, though rifampin is given only in combination therapies due to high rates of resistance development.[5] MRSA isolates resistant to vancomycin, daptomycin, and linezolid have already been observed in the clinic,[6–8] and high rates of adverse reactions to linezolid further complicate treatment.[9] There is therefore a need for safe, orally available anti-MRSA compounds with novel antimicrobial mechanisms to which resistance has not yet been observed.

Traditional methods for identifying new antibiotics include screening libraries of compounds for growth inhibition, but frequently fail to produce promising hits.[10] Heavily-exploited historic techniques including screening soil extracts for natural products rarely uncover novel molecules, while high-throughput screening using *in vitro* targets often fails to produce hits with significant activity in whole-cell assays.[11,12] One way to increase the likelihood of uncovering hit compounds is by using bioactive molecules, including drugs approved for non-antibiotic indications, since hit rates are significantly higher.[13] To increase our chances of identifying new antimicrobials, we developed a biofilm-based assay for high-throughput screening of previously-approved drugs and compounds with known bioactivity. Formation of *P. aeruginosa* biofilms – surface-associated communities of bacteria encased in a self-produced extracellular matrix – acts as a sensitive proxy for detecting antimicrobial activity, since it is stimulated in a dose-dependent manner by sub-inhibitory concentrations of antibiotics.[14] The biofilm stimulation phenotype allows us to screen compounds for growth inhibition at a low concentration of 10 μM, while alerting us to compounds that may have antibiotic activity above this concentration. Compounds with weaker antibiotic activity can then be improved through medicinal chemistry optimization, ensuring we miss fewer potential hits.

Using a biofilm stimulation screen, we identified the anti-inflammatory BAY 11-7082 as having antibacterial activity against multiple species, including MRSA. BAY 11-7082 is a synthetic anti-inflammatory that inhibits the nuclear factor-κB (NF-κB) pathway and the NLR Family Pyrin Domain Containing 3 (NLRP3)/caspase-1 inflammasome.[15,16] It is proposed to act by blocking IκB-α phosphorylation but may have alternate cellular targets, and its exact mechanism of action remains unknown.[15,17] BAY 11-7082 has also been proposed to act on mammalian protein tyrosine phosphatases (PTPs), which are involved in numerous cellular processes.[18] We re-synthesized BAY 11-7082 and began a medicinal chemistry effort to optimize its anti-*Staphylococcal* activity and determine the compound's structure-activity relationship (SAR). We ultimately transitioned to a related scaffold, 3-(phenylsulfonyl)-

93 2-pyrazinecarbonitrile (PSPC) and identified 10 analogues with improved anti-MRSA activity, validating
94 the utility of biofilm stimulation as a tool for novel antibiotic discovery.
95

96 Results

97 **BAY 11-7082 stimulates *P. aeruginosa* biofilm formation and has potent anti-MRSA activity**
98 Using a previously described biofilm assay,[19,20] we screened a library of 3,921 FDA approved or
99 biologically active compounds. Compounds were screened in duplicate at 10 μM against *P. aeruginosa*
100 PAO1 in a dilute media comprising 10% lysogeny broth (LB), 90% phosphate buffered saline (PBS)
101 (hereafter 10% LB). The screen yielded 60 compounds that inhibited *P. aeruginosa* growth to less than
102 50% of the vehicle (DMSO) control, 8 that inhibited biofilm formation to less than 50% of the control,
103 and 60 that stimulated biofilm formation above 200% of the control.[20] One of these biofilm stimulators
104 was the anti-inflammatory BAY 11-7082 **1** (Figure 1A), which we further explored due to its previously
105 unreported antibacterial activity. Using a dose-response assay (Figure 1B), we confirmed that BAY 11-
106 7082 stimulated *P. aeruginosa* biofilm formation at low concentrations and inhibited growth at higher
107 concentrations.
108
109 To explore its antibacterial potency and spectrum of activity, we determined the minimal inhibitory
110 concentration (MIC) in 10% LB for *P. aeruginosa* plus six other model and priority pathogens: *A.*
111 *baumannii*, *Bacillus subtilis*, *Escherichia coli*, *K. pneumoniae*, and two strains of MRSA (*S. aureus*
112 15981 and USA300) (Figure 1C). While BAY 11-7082 displayed modest activity against *P. aeruginosa*
113 (MIC: 100 μM, 20.73 μg/mL) and other Gram-negatives, it was particularly potent against Gram-
114 positives, including MRSA (MIC: 0.78 μM, 0.16 μg/mL), leading us to focus our efforts on developing
115 BAY 11-7082 as an anti-*Staphylococcal* agent. We also determined the MIC in two standard nutrient-rich
116 growth media, LB and Mueller-Hinton Broth (MHB) (Supplementary Figure 1). Based on the MIC in
117 MHB, we selected *S. aureus* 15981 over *S. aureus* USA300 as the strain of choice for comparing
118 synthetic analogues, since the lower baseline MIC would allow us to see a greater range of activities.
119
120 To test whether BAY 11-7082 has activity against drug-resistant strains, we exploited its modest activity
121 against *E. coli* to test it against the Antibiotic Resistance Platform (ARP),[21] a collection of
122 hyperpermeable efflux deficient *E. coli* BW25113 Δ*bamB*Δ*tolC* strains carrying genes that confer
123 resistance to a wide variety of antibiotics. A subset of the ARP was pinned onto Mueller Hinton Agar
124 (MHA) containing BAY 11-7082 at 25, 50, or 100 μM (Supplementary Figure 2). None of the *E. coli*
125 hyperpermeable strains were able to grow at concentrations as low as 25 μM (5.18 μg/mL), indicating
126 that BAY 11-7082 is an effective antibiotic even in the presence of common resistance elements.

127

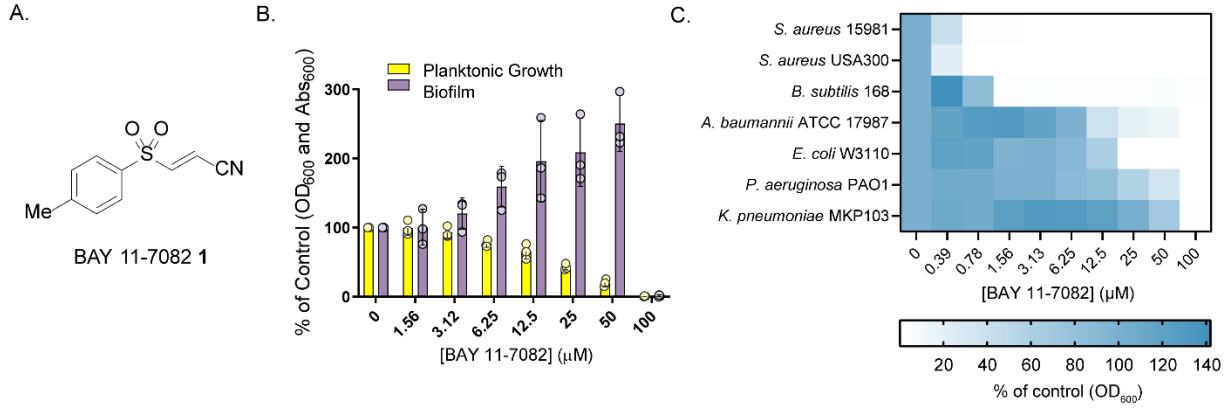

128

129 **Figure 1.** BAY 11-7082 **1** stimulates biofilm formation and has broad-spectrum antibacterial activity. (A)
130 Structure of BAY 11-7082. (B) BAY 11-7082 stimulates biofilm formation (absorbance of crystal violet
131 at 600 nm as a percent of the DMSO control) and decreases planktonic growth (optical density at 600 nm
132 as a percent of the DMSO control) of *P. aeruginosa* PAO1 in 10% LB. (C) BAY 11-7082 inhibits
133 planktonic growth (optical density at 600 nm as a percent of the DMSO control) of seven bacterial species
134 in 10% LB. Heatmap represents an average of three independent experiments performed in triplicate.

135

136 **Synthesis and antibacterial activity of analogues**

137 To improve potency and better understand the molecule's SAR, we synthesized a series of 15 informative
138 structural analogues (Figure 2) and evaluated them for anti-MRSA activity. Analogues **5-18** were
139 synthesized following General Procedure A (Supplementary Information), where a sodium sulfinate **2**
140 was combined with 2,3-dibromopropane nitrile, carboxamide or methyl ester **3** to allow for installation of
141 the alkene and the nitrile, or an alternate electron withdrawing group, on the right side of the molecule.
142 Analogues were designed with modifications to the left and/or right sides, including those with alternate
143 heterocycles or alternate substituents on the benzene ring on the left side (**5-8**, **10-16**, **18**, **19**) and those
144 with alternate electron withdrawing groups on the right side (**7**, **9-11**, **13-18**). Included in this group of
145 analogues is BAY 11-7085 **6** which, like BAY 11-7082, has reported anti-inflammatory activity.[15] To
146 determine if the alkene is essential for antimicrobial activity, which would suggest the mechanism
147 requires irreversible binding to a target at that position, we synthesized **19** through hydrogenation over
148 palladium on carbon of the potent analogue **5**.

149

150 Only **5** and **6** had improved potency against MRSA compared to BAY 11-7082. Moving from a methyl
151 group to the fluorine **5** or tert-butyl **6** increased potency. Similarly, **8**, which lacked substituents on the

benzene ring, was less potent than BAY 11-7082. With the surprising exception of **7**, analogues with substituents larger than a tert-butyl group, including the bicyclic heterocycles, had reduced potency, potentially due to steric hinderance at the molecular target(s). All other analogues with a non-nitrile group on the right side of the molecule were less active, leading us to conclude the nitrile is necessary for potent antimicrobial activity. As expected, **19** lacked antimicrobial activity up to the highest concentration tested of 100 µM.

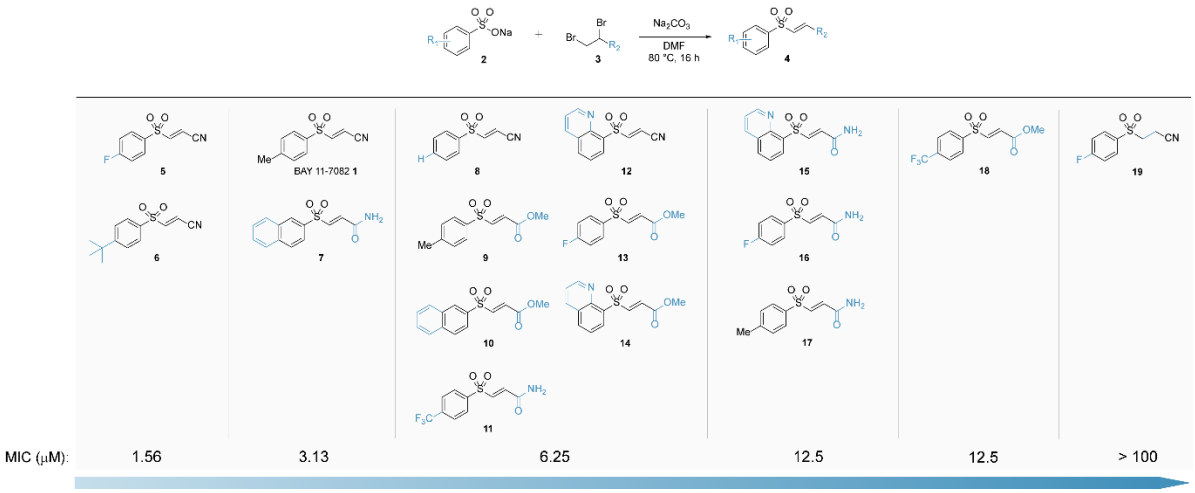

Figure 2. Synthesis (top) and antibacterial activity (bottom) of BAY 11-7082 **1** and its analogues **5-19**. Structures are arranged in order of increasing MIC values, reported in µM for *S. aureus* 15981 grown in MHB.

To further explore the molecule's SAR, we transitioned to a similar scaffold with an additional ring, offering new sites for diversification. We selected 3-(phenylsulfonyl)-2-pyrazinecarbonitrile (PSPC) **20** due to its structural similarities to BAY 11-7082 and its reported *in vivo* activity against MRSA in a *Caenorhabditis elegans* nematode infection model.[22] This scaffold also had the advantage of lacking the αβ-unsaturated sulfone in BAY 11-7082 that could lead to toxicity. We first confirmed that PSPC stimulated *P. aeruginosa* biofilm formation and had a similar spectrum of antibacterial activity, including potent activity against MRSA (Supplementary Figure 3), then synthesized the analogues **24-34** following General Procedure B (Supplementary Information), where a chlorocarbonitrile pyrazine or pyridine **21** was combined with a sulfonyl chloride **22** (Figure 3). PSPC differs from BAY 11-7082 by the addition of a pyrazine between the sulfone and the nitrile. While all analogues retain the nitrile group, some have a pyridine instead of a pyrazine (**33**, **34**). Capitalizing on our success with the fluorine analogue **5**, we designed analogues with halogen substituents at the para position of the benzene (**24**, **25**, **28**, **33**, **34**), as

well as **30** with a meta fluorine, three analogues with two fluorine substituents at differing positions (**27**, **31**, **32**), and **26** with a para trifluoromethyl group. We also explored a nitrile group (**29**) as an example of a non-halogen para electron withdrawing substituent.

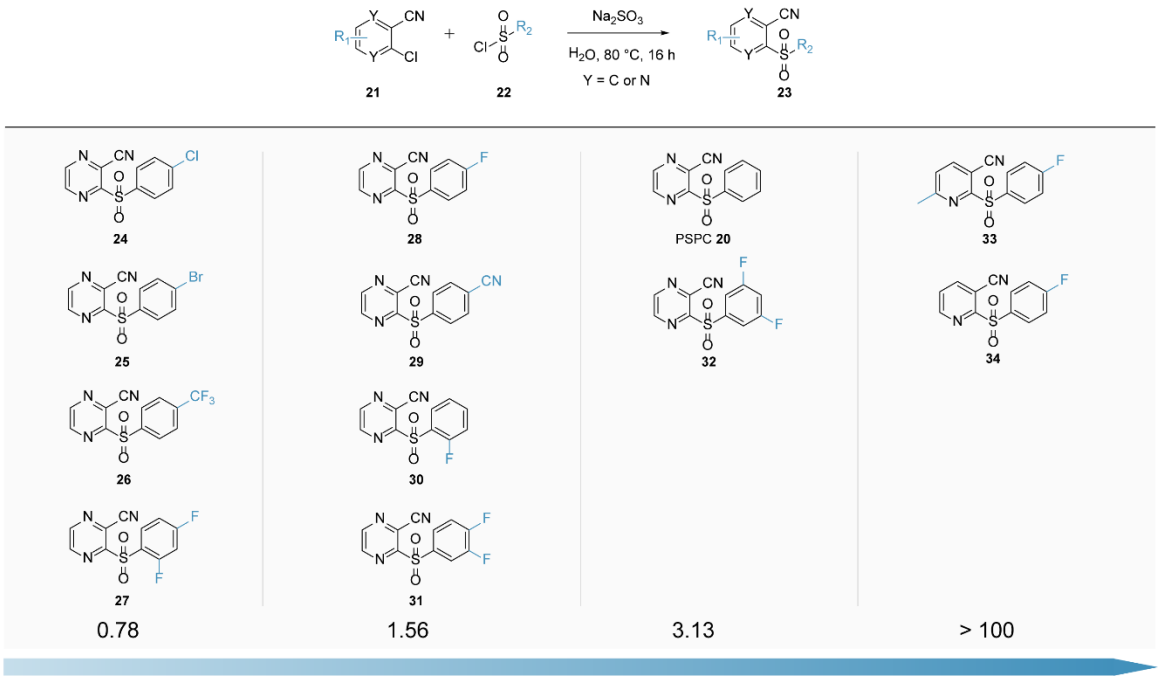

Figure 3. Synthesis (top) and antibacterial activity (bottom) of PSPC **20** and its analogues **24-34**. Structures are arranged in order of increasing MIC values reported in μM for *S. aureus* 15981 grown in MHB.

Analogues **24-31** all exhibited increased anti-MRSA activity relative to BAY 11-7082 and their parent compound PSPC, with MICs as low as 0.78 μM. Similar to our results with the first series of analogues, the addition of a halogen or other relatively small electron withdrawing substituent on the benzene ring increased potency, though the number or position of these groups had little impact. Pyridine analogues **33** and **34** lack antibacterial activity up to the highest concentration tested of 100 μM, indicating that while the pyrazine itself is not necessary for antibacterial activity – as in BAY 11-7082 and analogues **5-14** – the addition of a more basic heterocycle abrogates activity.

Evolving mutants resistant to BAY 11-7082 and PSPC

To understand BAY 11-7082 and PSPC's mechanism of action (MOA) and determine whether the two scaffolds shared a common target, we attempted to evolve resistant mutants of *S. aureus* 15981. While we

197 initially isolated colonies grown on MHA using supra-MIC (6X and 8X MIC) concentrations of BAY 11-
198 7082, those colonies did not grow when re-streaked on fresh MHA containing the compounds. We were
199 similarly unable to develop spontaneous resistance in *E. coli* or *A. baumannii*. We had more success
200 developing resistant mutants by serially passaging *S. aureus* 15981 cultures in liquid media containing
201 ~0.5X, ~1X MIC, or ~2X MIC concentrations of BAY 11-7082 or PSPC for 14 days. After purification of
202 resistant mutants on MHA, six colonies were selected for further evaluation, all of which displayed a 4-
203 fold increase in MIC compared to the parent strain (Figure 4A). Mutants selected using BAY 11-7082
204 displayed cross-resistance to PSPC and vice versa, suggesting that these two compounds act via a
205 conserved antibacterial mechanism (Figure 4B). To test whether resistance was retained in the absence of
206 selective pressure, the six mutants were serially passaged in MHB for five days and the compounds' MIC
207 was recorded each day. Over five days there was no decrease in MIC, indicating resistance is stably
208 inherited (Figure 4C). In growth experiments, all six mutants showed shorter lag times and increased final
209 optical density over 16 hours compared to the unpassaged parent strain ($p < 0.0001$) (Figure 4D), perhaps
210 due to a general increase in fitness resulting from passage. To ensure these mutants did not have elevated
211 antibiotic tolerance in general, we determined the MICs to tetracycline and piperacillin, and both were
212 unchanged in the mutants compared to the parent strain (Supplementary Figure 4). To identify the genetic
213 changes responsible for these mutants' resistance to BAY 11-7082 and PSPC, we purified and sequenced
214 genomic DNA from the parent strain *S. aureus* 15981 and the six mutants. Unexpectedly, the mutants
215 lacked shared genetic changes that could be associated with the acquisition of resistance (Supplementary
216 Table 1), forcing us to pursue other strategies to better understand the antibacterial MOA.

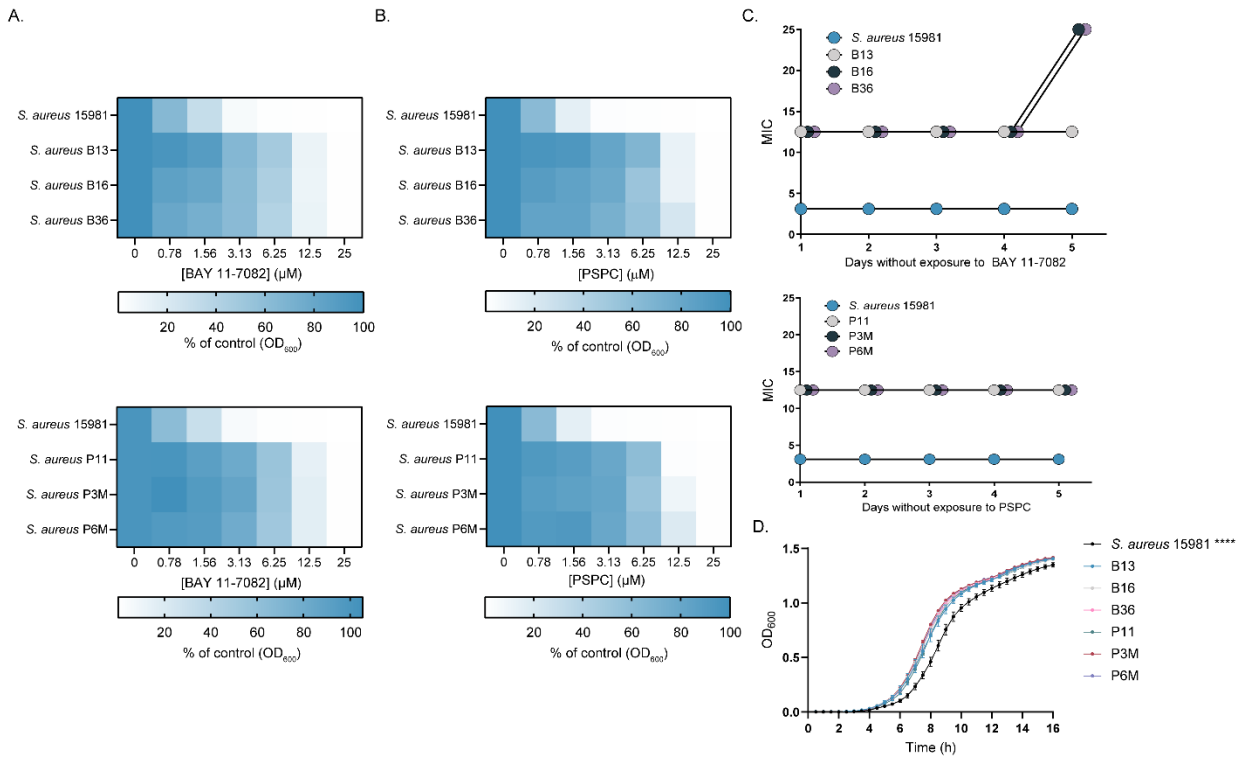

Figure 4. Mutants resistant to BAY 11-7082 and PSPC. (A) Planktonic growth (optical density at 600 nm as a percent of the DMSO control) of *S. aureus* 15981 and BAY 11-7082- (top) or PSPC-resistant (bottom) mutants grown with increasing concentrations of the compound used for selection. (B) Planktonic growth (optical density at 600 nm as a percent of the DMSO control) of *S. aureus* 15981 and BAY 11-7082- (top) or PSPC-resistant (bottom) mutants grown with increasing concentrations of the other compound. (C) MIC values for *S. aureus* 15981 or resistant mutants determined each day for five days during serial passage in the absence of compound. (D) Planktonic growth (optical density at 600 nm) of *S. aureus* 15981 or resistant mutants over 16 h. **** $p<0.0001$.

Exploring inhibition of TAT secretion as a potential mechanism

BAY 11-7082 was previously identified as a hit in a screen for inhibitors of the *P. aeruginosa* twin arginine translocase (TAT) system, a Sec-independent protein export system responsible for transporting folded proteins across the cytoplasmic membrane.[23] While TAT is not essential,[24,25] we were curious whether BAY 11-7082 would inhibit the *S. aureus* TAT system and if this would provide insight into its antibacterial mechanism. The TAT system is broadly conserved in prokaryotes but its protein composition varies between species, with the *P. aeruginosa* TAT system comprising three genes (*tatA*, *tatB*, and *tatC*) while the *S. aureus* system comprises two (*tatA* and *tatC*), with *tatA* and *tatC* essential for protein translocation in both species.[26,27] We determined the potency of BAY 11-7082 and PSPC against *tatC*

236 transposon mutants of *P. aeruginosa* PA14, from the PA14NR Set transposon mutant library,[28] and *S.*
237 *aureus* USA300, from the Nebraska transposon mutant library,[29] and saw a 2-fold increase in sensitivity
238 to BAY 11-7082 and PSPC relative to wild type only for *P. aeruginosa* (Figure 5). This was consistent
239 with the fact that we saw no genetic changes in TAT-related genes in the BAY 11-7082 and PSPC-
240 resistant mutants of MRSA and allowed us to rule out involvement of the TAT system or proteins
241 exported by the system in the compounds' MOA.

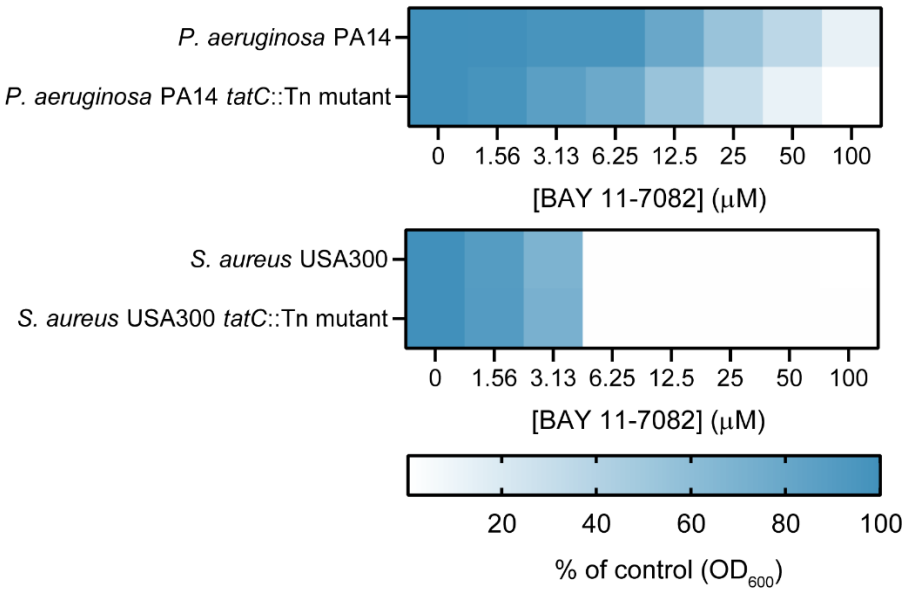

242

243 **Figure 5.** Planktonic growth (optical density at 600 nm as a percent of the DMSO control) of the parent
244 strain *P. aeruginosa* PA14 and a *tatC* transposon mutant grown in 10% LB (top) or the parent strain *S.*
245 *aureus* USA300 and a *tatC* transposon mutant grown in MHB (bottom) in the presence of increasing
246 concentrations of BAY 11-7082.

247

248 **Insight into BAY 11-7082's uptake and effect on the proton motive force**

249 Given the challenges of isolating BAY 11-7082- and PSPC-resistant mutants and our inability to isolate
250 mutants with greater than a 4-fold increase in MIC, plus the lack of consistent genetic changes in the
251 mutants isolated, we wondered if BAY 11-7082 and PSPC had a more general MOA, such as perturbation
252 of the proton motive force (PMF). The PMF has two components, a proton gradient (ΔpH) and an electric
253 potential (Δψ), which the cell coordinates to control the electrochemical gradient across the membrane.[30]
254 To test this idea, we determined the MIC of BAY 11-7082 and PSPC against *S. aureus* 15981 in pH
255 adjusted MHB (Figure 6A). Both BAY 11-7082 and PSPC displayed reduced potency in more basic
256 conditions and increased potency in more acidic conditions, similar to tetracycline, which is taken up via

257 the ΔpH component,[31] suggesting that BAY 11-7082 and PSPC may also experience ΔpH-dependent
258 uptake across the cytoplasmic membrane.
259
260 To determine if BAY 11-7082 and PSPC affected the PMF, we used 3,3'-dipropylthiadicarbocyanine
261 iodide ($DiSC_3(5)$), a fluorescent dye sensitive to PMF perturbations (Figure 6B). The dye is taken up and
262 transported to the cytoplasm via the Δψ component, where it accumulates and self-quenches fluorescence.
263 If Δψ is inhibited, dye does not accumulate, resulting in increased fluorescence, while if ΔpH is inhibited,
264 the cell compensates by increasing flux through Δψ, resulting in decreased fluorescence. Valinomycin,
265 nigericin, and carbonyl cyanide m-chlorophenyl hydrazine (CCCP) all dissipate the PMF and were used
266 as positive controls. Unlike the controls ($p<0.0001$), neither BAY 11-7082 nor PSPC significantly altered
267 $DiSC_3(5)$ fluorescence ($p>0.9999$), confirming that while their uptake is PMF-dependent, they themselves
268 do not destabilize the PMF.
269

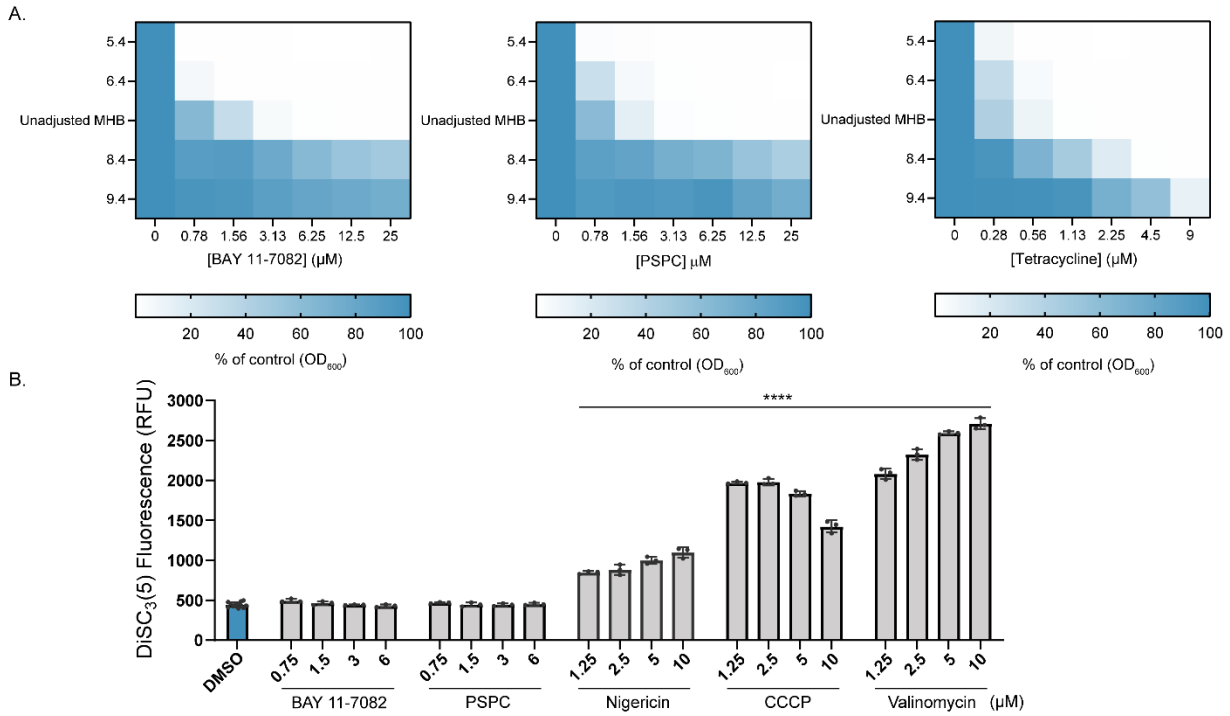

270
271 **Figure 6.** (A) Planktonic growth (optical density at 600 nm as a percent of the DMSO control) of *S.*
272 *aureus* 15981 grown in pH adjusted MHB with increasing concentrations of BAY 11-7082 (left), PSPC
273 (center), or tetracycline (right). Y-axis indicates pH of the media. (B) $DiSC_3(5)$ fluorescence in relative
274 fluorescence units of *S. aureus* USA300 in the presence of the vehicle DMSO, BAY 11-7082, PSPC, or
275 the membrane active controls nigericin, CCCP, or valinomycin. **** $p<0.0001$.
276

277 **BAY 11-7082 synergizes with multiple classes of antibiotics**

278 We next looked at whether BAY 11-7082 and its analogues could act as adjuvants to potentiate the
279 activity of other antibiotics. We conducted checkerboard experiments using the clinically-relevant MRSA
280 strain *S. aureus* USA300. It should be noted that the MIC for BAY 11-7082 and its analogues were ~4-
281 fold higher for *S. aureus* USA300 than the MICs for *S. aureus* 15981 reported in Schemes 2 and 3. Using
282 the fractional inhibitory concentration index (FICI), where values < 0.5 represent synergy and values > 4
283 represent antagonism,[32] we determined that BAY 11-7082 synergized with the β-lactam antibiotics
284 penicillin G and piperacillin, the RNA polymerase inhibitor rifampin, and the translation inhibitor
285 thiostrepton (Figure 7A). BAY 11-7082 did not affect the activity of antibiotics dependent on the PMF for
286 uptake, including tetracycline (ΔpH-dependent) and gentamicin (Δψ-dependent) (Figure 7A), consistent
287 with our observations that it does not alter the PMF. BAY 11-7082 did not synergize with the
288 glycopeptide cell wall synthesis inhibitor vancomycin or the β-lactam methicillin, to which *S. aureus*
289 USA300 is intrinsically resistant (Figure 7A). Given that we saw the strongest synergy between BAY 11-
290 7082 and penicillin G, we tested some of our more potent analogues in combination with that β-lactam.
291 We selected the BAY 11-7082 para-fluorine analogue **5** (MIC for *S. aureus* USA300: 12.5 μM) and the
292 para-bromine and para-trifluoromethyl PSPC analogues **25** and **26** (MICs for *S. aureus* USA300: 6.25
293 μM); both potentiated penicillin G activity to the same degree as BAY 11-7082 (FICI: 0.19) (Figure 7B).
294

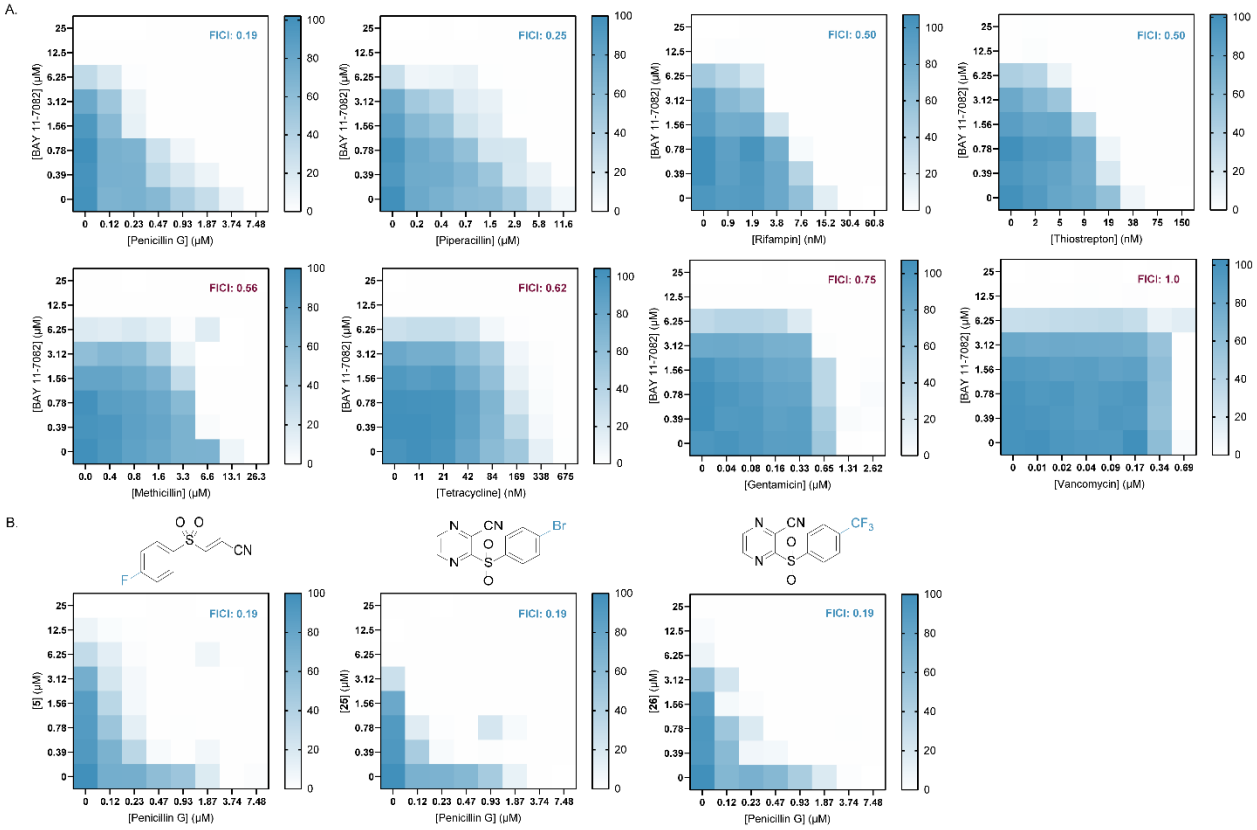

Figure 7. Checkerboards of *S. aureus* USA300 planktonic growth (optical density at 600 nm as a percent of the DMSO control) grown in MHB with increasing concentrations of BAY 11-7082 (A) or its analogues **5**, **25**, or **26** (B) with antibiotics of different classes. Synergy (FICI<0.5) is represented in blue text while indifference (FICI>0.5) is represented in red. Checkerboards represent an average of at least three independent experiments.

Anti-inflammatory properties of BAY 11-7082 and its analogues

Since the original BAY 11-7082 compound has anti-inflammatory activity, we tested whether alterations to the scaffold would allow us to separate its anti-inflammatory and antimicrobial properties. We treated mouse bone marrow-derived macrophages with *E. coli* O111:B4 lipopolysaccharide (LPS) and nigericin and measured IL-1β production, a key effector cytokine produced by priming and activating the NLRP3/caspase-1 inflammasome, in the presence or absence of BAY 11-7082 and four analogues (**5**, **12**, **17**, and **19**) (Figure 8). As expected, treatment with BAY 11-7082 at 1 and 2.5 μM significantly reduced ($p<0.0001$) IL-1β production compared to the no-treatment control. The potent antimicrobial **5** caused a similar reduction in IL-1β production at both 1 ($p=0.0057$) and 2.5 ($p<0.0001$) μM, as did the weaker antimicrobials **12** ($p<0.0001$) and **17** ($p<0.0001$). As expected, there was no significant difference in IL-

313 1β production between treatment with **19** – which lacks antimicrobial activity due to the reduction of the
314 alkene – at 2.5 μM versus the no-treatment control (p=0.5600), while treatment with 1 μM resulted in a
315 significant increase in IL-1β production (p=0.0061), supporting our notion that covalent binding is
316 required for the scaffold's anti-inflammatory activity. Surprisingly, treatment with **17**, which has an MIC
317 4-fold higher than that of BAY 11-7082, resulted in a greater, though not significant (p>0.9999),
318 reduction in IL-1β production at 2.5 μM compared to BAY 11-7082, indicating the terminal nitrile is not
319 required for anti-inflammatory potency. This result suggests that while it may not be possible to develop a
320 potent antimicrobial that does not also target the inflammasome, there may be room to develop a potent
321 anti-inflammatory compound with a reduced impact on the microbiome.

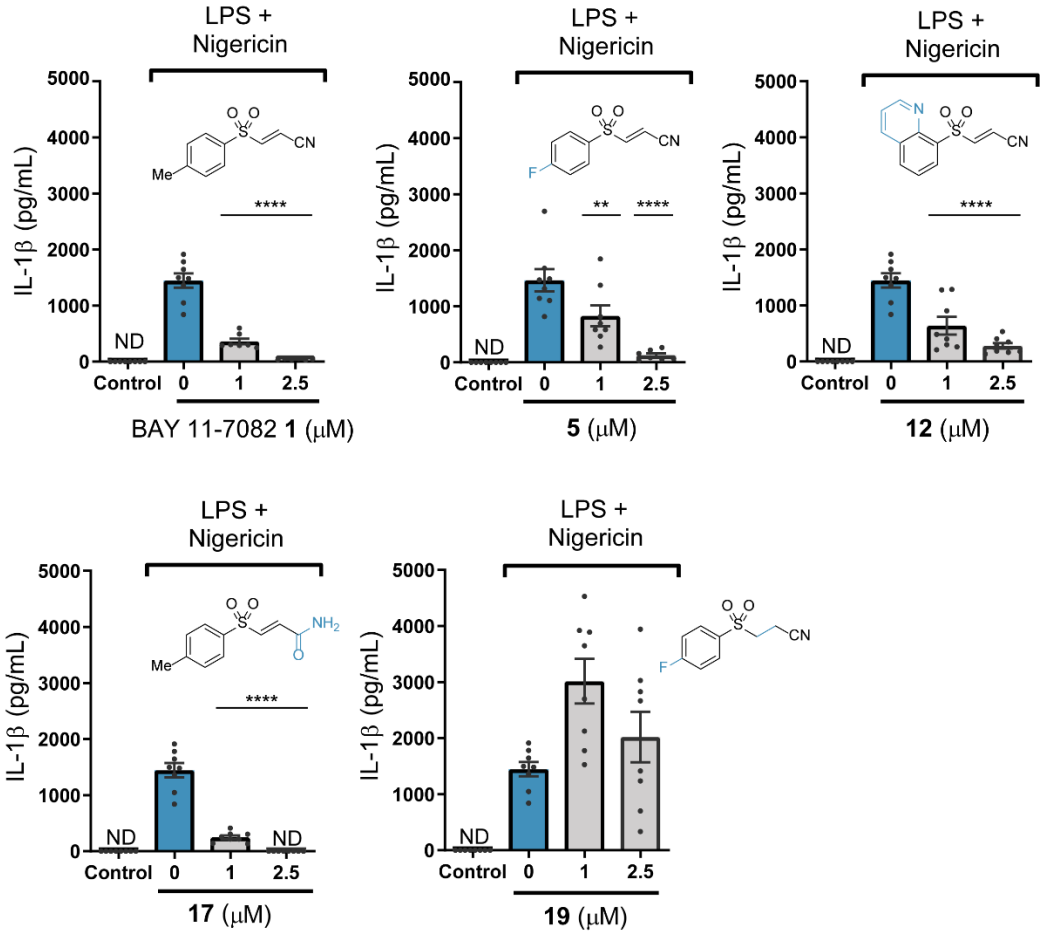

322
323

324 **Figure 8.** Production of IL-1β by bone marrow-derived macrophages stimulated with 200 ng/mL LPS and
325 10 μM nigericin in the presence or absence of BAY 11-7082, or the analogue **5**, **12**, **17**, or **19** at 1 or 2.5
326 μM. Control cells did not receive stimulation with LPS and nigericin. ND (not detected) indicates IL-1β
327 levels for that condition were below the level of detection based on a standard curve generated for IL-1β
328 concentration. ** p<0.01, **** p<0.0001

329 ## Discussion

330 Biofilm stimulation occurs in response to exposure to sub-inhibitory concentrations of antibiotics,
331 independent of their MOA,[14,33] making it a useful tool with advantages over traditional growth assays.
332 The biofilm assay does not rely on growth inhibition at an arbitrary screening concentration, alerting us to
333 hits with potential MICs above the test concentration. Our previous work showed that *P. aeruginosa*
334 biofilm production is a useful proxy for antimicrobial activity, both for narrow spectrum anti-
335 *Pseudomonal* compounds and for broad range molecules like the antibiotic thiostrepton.[20] Here we
336 confirmed that *P. aeruginosa* biofilm stimulation by the anti-inflammatory BAY 11-7082 at 10 µM
337 signalled its antimicrobial activity against a variety of species, including MRSA.
338
339 BAY 11-7085 **6**, another anti-inflammatory and structural analogue of BAY 11-7082, was recently
340 identified as an antimicrobial with activity against *S. aureus* and *Candida albicans*.[34] Similar to our
341 findings, BAY 11-7085 lacked activity against *P. aeruginosa* and *K. pneumoniae* strains up to 276.7 µM,
342 and Escobar *et al*. were unable to isolate BAY 11-7085-resistant mutants of *S. aureus*. Using
343 vancomycin-resistant *S. aureus* VRS1, they found an MIC of 16 µM in MHB and showed that BAY 11-
344 7085 inhibited cell surface attachment and biofilm formation and eradicated established biofilms in brain
345 heart infusion broth media with 0.1% glucose. Interestingly, they did not report biofilm stimulation in
346 response to sub-MIC concentrations of BAY 11-7085.
347
348 When initially describing BAY 11-7082 and BAY 11-7085's anti-inflammatory activity, Pierce *et al*.
349 suggested they act via preventing IκB-α phosphorylation initiated by cytokines like tumor necrosis factor-
350 α (TNF-α), resulting in lower NF-κB activation and nuclear translocation, where it regulates transcription
351 of κB sequences with various roles in immunity, cell survival, and apoptosis. Pierce *et al*. proposed BAY
352 11-7082 and BAY 11-7085 could inhibit a protein tyrosine kinase upstream of IκB-α but did not propose
353 a specific target. Subsequent work showed that BAY 11-7082 binds and irreversibly inhibits mammalian
354 PTPs through nucleophilic attack by a cysteine in the enzyme's active site,[18] suggesting that BAY 11-
355 7082's antibacterial target could be a PTP. In bacteria, classical PTPs play roles in virulence and host
356 immune evasion, while low-molecular-weight PTPs are primarily involved in polysaccharide transport.[35]
357 *S. aureus* contains two low molecular weight PTPs, PtpA and PtpB, both of unknown function.[36] We also
358 considered the TAT system as a target, as BAY 11-7082 was previously identified as a *P. aeruginosa*
359 TAT inhibitor, where it was also suggested to bind a nucleophilic cysteine.[23] However, another study
360 reported that BAY 11-7082 failed to inhibit protein export via the *E. coli* TAT system.[37] Further, loss of
361 the TAT system in these species is not lethal,[24,25] incongruent with the antimicrobial activity of BAY 11-
362 7082, nor was its activity different in a *S. aureus* TAT mutant (Figure 3). Finally, we saw no insertions,

363 deletions, or single nucleotide polymorphisms in PTP or TAT-related genes in mutants with increased
364 resistance to BAY 11-7082 or PSPC (Supplementary Table 1), consistent with our conclusion that BAY
365 11-7082's antibacterial MOA is unrelated to either of these systems. Given our inability to identify a
366 molecular target for BAY 11-7082, we suggest that its mechanism is likely complex. While this may be
367 due in part to the potential promiscuity conferred by BAY 11-7082's αβ-unsaturated sulfonyl, this moiety
368 is absent in PSPC, suggesting it does not play a role in the compound's MOA.
369
370 The αβ-unsaturated center, characteristic of highly-reactive Michael acceptors, makes BAY 11-7082 an
371 unlikely drug candidate. Michael acceptors have traditionally been considered problematic in drug
372 development due to concerns that the compounds could irreversibly bind off-target proteins. However,
373 views on the suitability of Michael acceptors and other covalent modifiers as drugs are changing –
374 particularly in the anticancer space – with several recent examples of αβ-unsaturated carbonyls under
375 development.[38–41] Such compounds work best when the αβ-unsaturated carbonyl binds a known and
376 biologically-uncommon target, reducing the likelihood of irreversible covalent off-target binding. Despite
377 our efforts, we were unable to identify a specific molecular target for BAY 11-7082, suggesting the
378 compound enacts its antibacterial effect via multiple mechanisms. We were also unable to identify an
379 analogue of BAY 11-7082 lacking anti-inflammatory activity but retaining antibiotic potency. While dual
380 antibiotic-anti-inflammatory compounds are an interesting concept and, indeed, many antibiotics have
381 been shown to affect the inflammasome,[42] this raises concern for potential side effects. Research from the
382 Taunton lab aimed at developing reversible cysteine residue inhibitors showed that positioning a nitrile
383 group on olefins increases thiol reactivity reversibility, as does positioning electron withdrawing groups
384 at the α or β position of acrylonitriles.[43,44] It is important to note that with the exploration of PSPC and the
385 development of analogues **24-31**, we showed that the αβ-unsaturated center is not required for potent anti-
386 MRSA activity.
387
388 Beyond its anti-inflammatory activity, BAY 11-7082 has anticancer, anti-diabetes, and neuroprotective
389 properties.[45–48] It is thus noteworthy that its potent activity against Gram-positive species could prove
390 problematic should the compound be developed for one of these indications, as it has potential to impact
391 the microbiome. This is not uncommon among drugs with human targets. Indeed, a recent study found
392 24% of all human-directed drugs tested inhibited growth of at least one bacterial species common to the
393 microbiome.[49] We found that analogue **17**, a weak anti-*Staphylococcal*, maintains strong anti-
394 inflammatory activity, suggesting it could be possible to separate the activities through careful design.
395

396 Due to its potential off-target effects, perhaps a better use of this antibacterial scaffold would be as a lead
397 for adjuvants used in combination with β-lactams to treat MRSA infections. Although BAY 11-7082 did
398 not re-sensitize MRSA strain USA300 to methicillin, at 1.56 μM it reduced the MIC of penicillin G from
399 3.74 μM to 0.23 μM – a 16-fold reduction. This concentration of BAY 11-7082 is well below the 10 μM
400 reported IC_{50} for inhibition of IκB-α phosphorylation,[15] but above the concentration that significantly
401 reduced inflammation in our macrophage model (Figure 6) and the K_i for some mammalian PTPs,[18]
402 suggesting that even at the low concentrations afforded by combination therapy, using this scaffold may
403 result in off-target effects. The BAY 11-7082 analogue **5** and the PSPC analogues **25** and **26** also
404 synergized with penicillin G and can be used at even lower concentrations (0.78 μM for **7** and 0.39 μM
405 for **25** and **26**) than BAY 11-7082 to achieve the same 0.23 μM MIC for penicillin G. Both **25** and **26**
406 have the advantage of lacking the αβ-unsaturated center found in BAY 11-7082 and **5**, making them the
407 most promising candidates for development of antibacterial combination therapies.
408

409 # Conclusion

410 A high-throughput screen using *P. aeruginosa* biofilm stimulation as an indicator of antibacterial activity
411 led to identification of BAY 11-7082 as a broad-spectrum antimicrobial, with activity against multiple
412 priority pathogens, including MRSA. This work confirms biofilm stimulation as a useful screening
413 method for identifying compounds with broad activity. We were able to improve upon the potency of
414 BAY 11-7082 by switching to a new chemical scaffold based on the molecule PSPC, which lacks the αβ-
415 unsaturated center that may be associated with off-target effects and toxicity. Our analogues **25** and **26**
416 potentiate the activity of β-lactams like penicillin G to reduce the concentration needed to inhibit the
417 growth of MRSA. These two compounds therefore represent an interesting starting point for the
418 development of an antibacterial adjuvant for the treatment of MRSA.
419

420 # Methods

421 **Bacterial strains, culture conditions, and chemicals**

422 Bacterial strains used in this study include *P. aeruginosa* PAO1[50], *S. aureus* 15981,[51] *B. subtilis* 168,[52] *E.*
423 *coli* K-12 W3110[53], *A. baumannii* ATCC 17987[20], and *K. pneumoniae* MKP103.[54] *P. aeruginosa* PA14
424 and the Δ*tatC* transposon mutant were from the PA14NR Set transposon mutant library[28] and *S. aureus*
425 USA300 and the Δ*tatC* transposon mutant was from the Nebraska transposon mutant library.[29] Bacterial
426 cultures were grown in lysogeny broth (LB), 10% LB (10% LB, 90% 1X phosphate buffered saline), or
427 Mueller-Hinton broth (MHB). Solid media was solidified with 1.5% agar. Compounds **1**, **7-22**, and **26-37**
428 were synthesized for this work. One hundred mM stock solutions were made in DMSO and stored at -

429 20°C. Stock solutions of tetracycline (EMD Millipore), piperacillin (Sigma, 40 mg/mL stock solution),
430 penicillin G (Fluka Analytica), rifampin (Sigma, 1 mg/mL stock solution prepared in DMSO),
431 thiostrepton (Sigma, 5 mM stock solution prepared in DMSO), methicillin (Cayman Chemicals),
432 gentamicin (BioShops), and vancomycin (Sigma, stock solution prepared in DMSO) were prepared at 10
433 mg/mL in sterile de-ionized H_2O except where noted and stored at -20°C.
434
435 **Compound screening**
436 The McMaster Bioactive compound collection was screened using a biofilm modulation assay, as
437 previously described.[20]
438
439 **Inhibitory concentration assays**
440 All bacterial strains were inoculated from -80°C glycerol stocks into 5 mL media, and incubated with
441 shaking, 200 rpm, 37°C for 16 h. Cultures were sub-cultured in a 1:500 dilution, grown for 4 h, and
442 diluted in fresh media to an OD_{600} of ~ 0.1, then diluted 1:500. Minimal inhibitory concentration values
443 were determined in 96-well plates (Nunc) using compounds serially diluted in DMSO. Each well had a
444 final volume of 150 µL. Sterile control wells contained 148 µL of corresponding broth and 2 µL DMSO
445 while vehicle control wells contained 148 µL dilute bacterial culture and 2 µL DMSO. Plates were sealed
446 in a container and incubated with shaking, 200 rpm, 37°C, 16 h. The OD_{600} of plates was read using a
447 Multiscan GO (Thermo Fisher Scientific) and used to calculate the inhibitory concentration. All MIC
448 values presented in Scheme 1 and Scheme 2 were conducted with *S. aureus* 15981 grown in MHB and are
449 based on experiments performed in duplicate. All other inhibitory concentration data was conducted in
450 media as specified and is based on at least three independent experiments performed in triplicate. MIC
451 values were defined as < 20% of the vehicle control, where growth is no longer visible.[20] Where
452 specified, media was pH-adjusted using 6 N sodium hydroxide and 6 M hydrogen chloride.
453
454 **Biofilm modulation assays**
455 Biofilm assays were performed as previously described.[20] Briefly, *P. aeruginosa* PAO1 was inoculated
456 from -80°C glycerol stocks into 5 mL 10% LB, and incubated with shaking, 200 rpm, 37°C for 16 h.
457 Cultures were sub-cultured in a 1:500 dilution, grown for 4 h, and diluted in fresh media to an OD_{600} of ~
458 0.1, then diluted 1:500. Plates were set up as for the inhibitory concentration assays. Biofilms were
459 formed on the polystyrene pegs of MicroWell lids (Nunc), which were placed on assay plates prior to 16
460 h incubation with shaking, 200 rpm, 37°C. Following incubation, lids were removed and planktonic
461 growth (OD_{600}) was measured. Lids were immersed in 1X phosphate buffered saline and washed for 10
462 min, then biofilms adhering to the lids were stained in 0.1% crystal violet for 15 min. Excess crystal

463 violet was removed by immersing the lids in deionized water for 5 min, then repeating this wash step four
464 additional times. Lids dried for 1 h then were transferred to a new 96-well plate containing 200 µL 33.3%
465 acetic acid per well for 5 min to solubilize the crystal violet. The absorbance (Abs_{600}) of the 96-well plates
466 was read using a Multiscan GO (Thermo Fisher Scientific). Three independent experiments were
467 performed in triplicate and technical triplicates were averaged. The mean and standard error of the
468 independent biological replicates are shown.
469
470 **Liquid serial passage assays**
471 *S. aureus* 15981 was taken from -80°C stocks, inoculated into 5 mL MHB, and grown with shaking, 200
472 rpm, 37°C for 24 h. One hundred µL culture was inoculated into fresh MHB supplemented with BAY 11-
473 7082 or PSPC at 1 (B13, B16, and P11), 3 (B36, P3M), or 6 (P6M) µM and grown with shaking 200 rpm,
474 37°C for 24 h. One hundred µL culture was inoculated into fresh MHB supplemented with BAY 11-7082
475 or PSPC at the same concentration as the previous day. This serial liquid passage continued for 14 days,
476 at which point cultures were purified on MHA with or without compound.
477
478 **Genome assembly and identification of SNPs**
479 Genomic DNA was purified using the Wizard Genomic DNA purification kit (Promega) then sequenced
480 via Illumina sequencing. Quality control and trimming of sequencing reads was accomplished using
481 Galaxy through FASTQC for quality control, FASTQC Groomer to reformat reads, Trimmomatic to trim
482 poor quality reads, FASTQC Interlacer to reorder reads, and FASTQC De-Interlacter. Contigs were
483 assembled for the *S. aureus* 15981 genome using SPAdes and genomes were mapped to reference
484 genomes of two closely related species, *S. aureus* USA300 and USA500, using BreSeq.
485
486 **Growth Curves**
487 *S. aureus* 15981 and the six BAY 11-7082- or PSPC-resistant mutants (B13, B16, B36, P11, P3M, P6M)
488 were taken from -80°C stocks, inoculated into 2 mL MHB, and grown with shaking, 200 rpm, 37°C for
489 16 h. Overnight cultures were sub-cultured in a 1:500 dilution, grown for 4 h, and diluted in fresh media
490 to an OD_{600} of ~ 0.1, then diluted 1:500. Three replicates of 150 µL of each sample was added to a 96-
491 well plate and incubated with moderate shaking at 37°C (BioTek Synergy 4 Plate Reader) and the OD_{600}
492 was measured at 30 min intervals for 16 h. Technical replicates were averaged and the experiment was
493 repeated at least three times for each strain. The mean and standard error of the independent biological
494 replicates are shown. P-values were calculating using a one-way ANOVA and Tukey's multiple
495 comparison test.
496

497 **$DiSC_3(5)$ assays**

498 The $DiSC_3(5)$ assay was performed in accordance with modifications by Farha *et al*[55] to a method by
499 Epand *et al*[56], with some modifications. Briefly, *S. aureus* USA300 was taken from -80°C stock,
500 inoculated into 5 mL MHB, and grown with shaking, 200 rpm, 37°C for 16 h. Cultures were sub-cultured
501 in a 1:500 dilution and grown for 4 h. Cells were pelleted and washed three times in buffer (10 mM
502 potassium phosphate, 5 mM MgSO4, and 250 mM sucrose, pH 7.0), then resuspended in buffer to an
503 OD_{600} of 0.1. $DiSC_3(5)$ was added at 1 µM and allowed to stabilize at room temperature in the dark for 20
504 minutes. BAY 11-7082, PSPC, valinomycin, nigericin, and CCCP were diluted in DMSO and added in
505 triplicate to a white, clear-bottom, 96-well plate (Costar, Corning Inc), along with cells. Vehicle control
506 wells contained 2 µL DMSO and 148 µL bacteria suspended in buffer with dye. Fluorescence was
507 measured (BioTek Synergy 4 Plate Reader) at an excitation wavelength of 620 nm and an emission
508 wavelength of 685 nm at the start time, then every 50 s for 10 min and every 5 min for the next 30 min.
509 The mean and standard error of three technical replicates for each condition are plotted at the start time.
510 P-values were calculating using a one-way ANOVA and Tukey's multiple comparison test.

511

512 **Checkerboard assays**

513 Checkerboard assays were set up identically to inhibitory concentration assays, except compounds were
514 added to an 8x8 section of a 96-well plate with increasing concentrations of one compound across the X-
515 axis and increasing concentrations of the other compound across the Y-axis. Plates were incubated with
516 shaking, 200 rpm, 37°C, 16 h. The OD_{600} of plates was read using a Multiscan GO (Thermo Fisher
517 Scientific). At least three biological replicates were averaged for each checkerboard. Synergy was
518 determined using the following formular for fractional inhibitory concentration index (FICI), where
519 values < 0.5 represent synergy and values > 4 represent antagonism[32]:

520 $$\frac{\mathrm{MIC}_{\text{Compound A in combination}}}{\mathrm{MIC}_{\text{Compound A alone}}} + \frac{\mathrm{MIC}_{\text{Compound B in combination}}}{\mathrm{MIC}_{\text{Compound B alone}}}$$

521

522 **NLRP3 inflammasome assays**

523 In-house male wild type C57BL/6 J mice (Jackson Laboratory) aged four to twelve weeks were humanely
524 sacrificed to generate bone marrow derived macrophages (BMDMs), as previously described.[57] Briefly,
525 bone marrow was isolated by flushing the marrow cavity of the femur with sterile saline. Cells recovered
526 from femur flushes were propagated in tissue culture flasks at 1 x 10^6 cells/mL in L929 differentiation
527 media at 37°C for four days. Additional L929 media was added and cells were transferred to 24-well
528 plates and incubated for another 5-7 days to allow for maturation of BMDMs. L929 media was removed
529 from BMDMs, wells were washed with PBS, and Dulbecco's Modified Eagle Medium (DMEM) (600

530 μL) was added. BMDMs were treated with BAY 11-7082 or analogues at a final concentration of 1 and
531 2.5 μM and *E. coli* O111:B4 LPS diluted in endotoxin-free ultra pure water at a final concentration of 200
532 ng/mL and incubated at 37°C for 3 h. Nigericin diluted in DMEM was added at a final concentration of
533 10 μM and cells were incubated for an additional 45 min. Each condition was tested in at least six
534 biological replicates in BMDMs from a single mouse. Two hundred and fifty μL of media was removed
535 from each well and frozen until IL-1β secretion could be measured by ELISA, (DuoSet ELISA, Mouse
536 1L-1β/IL-1F2, R&D Systems), as previously described.[58] Media was diluted in a 1:10 ratio in ELISA
537 reagent dilute (1% BSA in PBS) for the LPS and nigericin condition and all test conditions. Media from
538 the control condition, which lacked LPS, nigericin, or the analogues, was diluted in a 1:1 ratio in ELISA
539 reagent dilute. Absorbance at 450 and 570 nm of the 96-well plate following ELISA was read and values
540 at 570 nm were subtracted from values at 450 nm to correct for optical imperfections. IL-1β levels
541 corresponding to the subtracted absorbance values were determined by interpolating from a standard
542 curve generated using IL-1β concentrations ranging from 0 pg/mL to 1000 pg/mL. The mean and
543 standard error for at least six independent biological replicates is shown. P-values were calculating using
544 a one-way ANOVA and Tukey's multiple comparison test.
545

546 Supporting Information

547 Antibacterial activity of BAY 11-7082 in rich media; activity of BAY 11-7082 against a collection of
548 bacterial strains containing common resistance elements; antibacterial and antibiofilm activity of PSPC;
549 growth of BAY 11-7082- and PSPC-resistant mutants in the presence of tetracycline and piperacillin;
550 synthetic schemes and characterization data (1H NMR, C13 NMR, and HRMS) for compounds 1, **5-20**,
551 and **24-34**.
552

553 Corresponding Author Information

554 Lori L. Burrows
555 lori.burrows@mcmaster.ca
556 MDCL 2238 – 1280 Main St. West,
557 Hamilton, ON L8S4K1 Canada
558

559 Author Contributions

560 VEC and HH completed antibacterial susceptibility testing. PD, XZ, and VEC completed chemical
561 synthesis, supervised by JM. VEC and BDH conducted the NLRP3 inflammasome assays, supervised by

562 JDS. VEC and AY compiled genetic data related to the resistant mutants. All other experiments were
563 performed by VEC. VEC and LLB wrote the paper, with input from JM and JDS.
564

565 Acknowledgements

566 We thank Gerry Wright for access to the Antibiotic Resistance Platform, Derek Chan and Kara Tsang for
567 their assistance with BreSeq, and Meghan Fragis for determining exact masses of the compounds. This
568 work was supported by grants from the Natural Sciences and Engineering Research Council (NSERC)
569 RGPIN-2016-06521 and Ontario Research Fund RE07-048 to LLB and a seed grant from the David
570 Braley Centre for Antibiotic Discovery to LLB and JM. The NMR machine was purchased with funding
571 from a Canada Foundation for Innovation grant. VEC was supported by a Summer Studentship from the
572 David Braley Centre for Antibiotic Discovery and a CIHR Canadian Graduate Scholarship – Master's
573 Award.
574

575 Abbreviations Used

576 ARP, Antibiotic Resistance Platform; CCCP, carbonyl cyanide m-chlorophenyl hydrazine; $DiSC_3(5)$,
577 3,3'-dipropylthiadicarbocyanine iodide; FICI, fractional inhibitory concentration index; LB, lysogeny
578 broth; MHA, Mueller-Hinton agar; MHB, Mueller-Hinton broth; PMF, proton motive force; PSPC, 3-
579 (phenylsulfonyl)-2-pyrazinecarbonitrile; PTP, protein tyrosine phosphatase; TAT, twin arginine
580 translocase
581

582 References

583 (1) Rice, L. B. Federal Funding for the Study of Antimicrobial Resistance in Nosocomial Pathogens:
584 No ESKAPE. *J. Infect. Dis.* **2008**, *197* (8), 1079–1081. https://doi.org/10.1086/533452.
585 (2) Boucher, H. W.; Talbot, G. H.; Bradley, J. S.; Edwards, J. E.; Gilbert, D.; Rice, L. B.; Scheld, M.;
586 Spellberg, B.; Bartlett, J. Bad Bugs, No Drugs: No ESKAPE! An Update from the Infectious
587 Diseases Society of America. *Clin. Infect. Dis.* **2009**, *48* (1), 1–12. https://doi.org/10.1086/595011.
588 (3) Spellberg, B.; Powers, J. H.; Brass, E. P.; Miller, L. G.; Edwards, J. E. Trends in Antimicrobial
589 Drug Development: Implications for the Future. *Clin. Infect. Dis.* **2004**, *38* (9), 1279–1286.
590 https://doi.org/10.1086/420937.
591 (4) Deak, D.; Outterson, K.; Powers, J. H.; Kesselheim, A. S. Progress in the Fight Against Multidrug-
592 Resistant Bacteria? A Review of U.S. Food and Drug Administration–Approved Antibiotics,
593 2010–2015. *Ann. Intern. Med.* **2016**, *165* (5), 363–372. https://doi.org/10.7326/M16-0291.

(5) Liu, C.; Bayer, A.; Cosgrove, S. E.; Daum, R. S.; Fridkin, S. K.; Gorwitz, R. J.; Kaplan, S. L.; Karchmer, A. W.; Levine, D. P.; Murray, B. E.; Rybak, M. J.; Talan, D. A.; Chambers, H. F. Clinical Practice Guidelines by the Infectious Diseases Society of America for the Treatment of Methicillin-Resistant *Staphylococcus aureus* Infections in Adults and Children. *Clin. Infect. Dis.* **2011**, *52* (3), e18–e55. https://doi.org/10.1093/cid/ciq146.

(6) Nannini, E.; Murray, B. E.; Arias, C. A. Resistance or Decreased Susceptibility to Glycopeptides, Daptomycin, and Linezolid in Methicillin-Resistant *Staphylococcus aureus*. *Curr. Opin. Pharmacol.* **2010**, *10* (5), 516–521. https://doi.org/10.1016/j.coph.2010.06.006.

(7) Tsiodras, S.; Gold, H. S.; Sakoulas, G.; Eliopoulos, G. M.; Wennersten, C.; Venkataraman, L.; Moellering, R. C.; Ferraro, M. J. Linezolid Resistance in a Clinical Isolate of *Staphylococcus aureus*. *The Lancet* **2001**, *358* (9277), 207–208. https://doi.org/10.1016/S0140-6736(01)05410-1.

(8) Boucher, H. W.; Sakoulas, G. Perspectives on Daptomycin Resistance, with Emphasis on Resistance in *Staphylococcus aureus*. *Clin. Infect. Dis.* **2007**, *45* (5), 601–608. https://doi.org/10.1086/520655.

(9) Bishop, E.; Melvani, S.; Howden, B. P.; Charles, P. G. P.; Grayson, M. L. Good Clinical Outcomes but High Rates of Adverse Reactions during Linezolid Therapy for Serious Infections: A Proposed Protocol for Monitoring Therapy in Complex Patients. *Antimicrob. Agents Chemother.* **2006**, *50* (4), 1599–1602. https://doi.org/10.1128/AAC.50.4.1599-1602.2006.

(10) Silver, L. L. Challenges of Antibacterial Discovery. *Clin. Microbiol. Rev.* **2011**, *24* (1), 71–109. https://doi.org/10.1128/CMR.00030-10.

(11) Lewis, K. The Science of Antibiotic Discovery. *Cell* **2020**, *181* (1), 29–45. https://doi.org/10.1016/j.cell.2020.02.056.

(12) Lewis, K. Platforms for Antibiotic Discovery. *Nat. Rev. Drug Discov.* **2013**, *12* (5), 371–387. https://doi.org/10.1038/nrd3975.

(13) Sateriale, A.; Bessoff, K.; Sarkar, I. N.; Huston, C. D. Drug Repurposing: Mining Protozoan Proteomes for Targets of Known Bioactive Compounds. *J. Am. Med. Inform. Assoc.* **2014**, *21* (2), 238–244. https://doi.org/10.1136/amiajnl-2013-001700.

(14) Ranieri, M. R.; Whitchurch, C. B.; Burrows, L. L. Mechanisms of Biofilm Stimulation by Subinhibitory Concentrations of Antimicrobials. *Curr. Opin. Microbiol.* **2018**, *45*, 164–169. https://doi.org/10.1016/j.mib.2018.07.006.

(15) Pierce, J. W.; Schoenleber, R.; Jesmok, G.; Best, J.; Moore, S. A.; Collins, T.; Gerritsen, M. E. Novel Inhibitors of Cytokine-Induced IκBα Phosphorylation and Endothelial Cell Adhesion Molecule Expression Show Anti-Inflammatory Effects in Vivo. *J. Biol. Chem.* **1997**, *272* (34), 21096–21103. https://doi.org/10.1074/jbc.272.34.21096.

628 (16) Juliana, C.; Fernandes-Alnemri, T.; Wu, J.; Datta, P.; Solorzano, L.; Yu, J.-W.; Meng, R.; Quong,
629 A. A.; Latz, E.; Scott, C. P.; Alnemri, E. S. Anti-Inflammatory Compounds Parthenolide and Bay
630 11-7082 Are Direct Inhibitors of the Inflammasome. *J. Biol. Chem.* **2010**, *285* (13), 9792–9802.
631 https://doi.org/10.1074/jbc.M109.082305.
632 (17) Lee, J.; Rhee, M. H.; Kim, E.; Cho, J. Y. BAY 11-7082 Is a Broad-Spectrum Inhibitor with Anti-
633 Inflammatory Activity against Multiple Targets. *Mediators Inflamm.* **2012**.
634 https://doi.org/10.1155/2012/416036.
635 (18) Krishnan, N.; Bencze, G.; Cohen, P.; Tonks, N. K. The Anti-Inflammatory Compound BAY-11-
636 7082 Is a Potent Inhibitor of Protein Tyrosine Phosphatases. *FEBS J.* **2013**, *280* (12), 2830–2841.
637 https://doi.org/10.1111/febs.12283.
638 (19) Wenderska, I. B.; Chong, M.; McNulty, J.; Wright, G. D.; Burrows, L. L. Palmitoyl-Dl-Carnitine
639 Is a Multitarget Inhibitor of *Pseudomonas aeruginosa* Biofilm Development. *ChemBioChem* **2011**,
640 *12* (18), 2759–2766. https://doi.org/10.1002/cbic.201100500.
641 (20) Ranieri, M. R. M.; Chan, D. C. K.; Yaeger, L. N.; Rudolph, M.; Karabelas-Pittman, S.; Abdo, H.;
642 Chee, J.; Harvey, H.; Nguyen, U.; Burrows, L. L. Thiostrepton Hijacks Pyoverdine Receptors To
643 Inhibit Growth of *Pseudomonas aeruginosa*. *Antimicrob. Agents Chemother.* **2019**, *63* (9).
644 https://doi.org/10.1128/AAC.00472-19.
645 (21) Cox, G.; Sieron, A.; King, A. M.; Pascale, G. D.; Pawlowski, A. C.; Koteva, K.; Wright, G. D. A
646 Common Platform for Antibiotic Dereplication and Adjuvant Discovery. *Cell Chem. Biol.* **2017**,
647 *24* (1), 98–109. https://doi.org/10.1016/j.chembiol.2016.11.011.
648 (22) Rajamuthiah, R.; Jayamani, E.; Majed, H.; Conery, A. L.; Kim, W.; Kwon, B.; Fuchs, B. B.;
649 Kelso, M. J.; Ausubel, F. M.; Mylonakis, E. Antibacterial Properties of 3-(Phenylsulfonyl)-2-
650 Pyrazinecarbonitrile. *Bioorg. Med. Chem. Lett.* **2015**, *25* (22), 5203–5207.
651 https://doi.org/10.1016/j.bmcl.2015.09.066.
652 (23) Vasil, M. L.; Tomaras, A. P.; Pritchard, A. E. Identification and Evaluation of Twin-Arginine
653 Translocase Inhibitors. *Antimicrob. Agents Chemother.* **2012**, *56* (12), 6223–6234.
654 https://doi.org/10.1128/AAC.01575-12.
655 (24) Biswas, L.; Biswas, R.; Nerz, C.; Ohlsen, K.; Schlag, M.; Schäfer, T.; Lamkemeyer, T.; Ziebandt,
656 A.-K.; Hantke, K.; Rosenstein, R.; Götz, F. Role of the Twin-Arginine Translocation Pathway in
657 *Staphylococcus*. *J. Bacteriol.* **2009**, *191* (19), 5921–5929. https://doi.org/10.1128/JB.00642-09.
658 (25) Ochsner, U. A.; Snyder, A.; Vasil, A. I.; Vasil, M. L. Effects of the Twin-Arginine Translocase on
659 Secretion of Virulence Factors, Stress Response, and Pathogenesis. *Proc. Natl. Acad. Sci.* **2002**, *99*
660 (12), 8312–8317. https://doi.org/10.1073/pnas.082238299.

661 (26) Yen, M.-R.; Tseng, Y.-H.; Nguyen, E. H.; Wu, L.-F.; Saier, M. H. Sequence and Phylogenetic
662 Analyses of the Twin-Arginine Targeting (Tat) Protein Export System. *Arch. Microbiol.* **2002**, *177*
663 (6), 441–450. https://doi.org/10.1007/s00203-002-0408-4.
664 (27) Dilks, K.; Rose, R. W.; Hartmann, E.; Pohlschröder, M. Prokaryotic Utilization of the Twin-
665 Arginine Translocation Pathway: A Genomic Survey. *J. Bacteriol.* **2003**, *185* (4), 1478–1483.
666 https://doi.org/10.1128/JB.185.4.1478-1483.2003.
667 (28) Liberati, N. T.; Urbach, J. M.; Miyata, S.; Lee, D. G.; Drenkard, E.; Wu, G.; Villanueva, J.; Wei,
668 T.; Ausubel, F. M. An Ordered, Nonredundant Library of *Pseudomonas aeruginosa* Strain PA14
669 Transposon Insertion Mutants. *Proc. Natl. Acad. Sci.* **2006**, *103* (8), 2833–2838.
670 https://doi.org/10.1073/pnas.0511100103.
671 (29) Fey, P. D.; Endres, J. L.; Yajjala, V. K.; Widhelm, T. J.; Boissy, R. J.; Bose, J. L.; Bayles, K. W. A
672 Genetic Resource for Rapid and Comprehensive Phenotype Screening of Nonessential
673 *Staphylococcus aureus* Genes. *mBio 4* (1), e00537-12. https://doi.org/10.1128/mBio.00537-12.
674 (30) Kashket, E. R. The Proton Motive Force in Bacteria: A Critical Assessment of Methods. *Annu.*
675 *Rev. Microbiol.* **1985**, *39* (1), 219–242. https://doi.org/10.1146/annurev.mi.39.100185.001251.
676 (31) Yamaguchi, A.; Ohmori, H.; Kaneko-Ohdera, M.; Nomura, T.; Sawai, T. Delta pH-Dependent
677 Accumulation of Tetracycline in *Escherichia coli*. *Antimicrob. Agents Chemother.* **1991**, *35* (1),
678 53–56. https://doi.org/10.1128/AAC.35.1.53.
679 (32) Odds, F. C. Synergy, Antagonism, and What the Chequerboard Puts between Them. *J. Antimicrob.*
680 *Chemother.* **2003**, *52* (1), 1–1. https://doi.org/10.1093/jac/dkg301.
681 (33) Townsley, L.; Shank, E. A. Natural-Product Antibiotics: Cues for Modulating Bacterial Biofilm
682 Formation. *Trends Microbiol.* **2017**, *25* (12), 1016–1026.
683 https://doi.org/10.1016/j.tim.2017.06.003.
684 (34) Escobar, I. E.; Possamai Rossatto, F. C.; Kim, S. M.; Kang, M. H.; Kim, W.; Mylonakis, E.
685 Repurposing Kinase Inhibitor Bay 11-7085 to Combat *Staphylococcus aureus* and *Candida*
686 *albicans* Biofilms. *Front. Pharmacol.* **2021**, *12*, 675300.
687 https://doi.org/10.3389/fphar.2021.675300.
688 (35) Böhmer, F.; Szedlacsek, S.; Tabernero, L.; Östman, A.; Hertog, J. den. Protein Tyrosine
689 Phosphatase Structure–Function Relationships in Regulation and Pathogenesis. *FEBS J.* **2013**, *280*
690 (2), 413–431. https://doi.org/10.1111/j.1742-4658.2012.08655.x.
691 (36) Soulat, D.; Vaganay, E.; Duclos, B.; Genestier, A.-L.; Etienne, J.; Cozzone, A. J. *Staphylococcus*
692 *aureus* Contains Two Low-Molecular-Mass Phosphotyrosine Protein Phosphatases. *J. Bacteriol.*
693 **2002**, *184* (18), 5194–5199. https://doi.org/10.1128/JB.184.18.5194-5199.2002.

694 (37) Bageshwar, U. K.; VerPlank, L.; Baker, D.; Dong, W.; Hamsanathan, S.; Whitaker, N.;
695 Sacchettini, J. C.; Musser, S. M. High Throughput Screen for *Escherichia coli* Twin Arginine
696 Translocation (Tat) Inhibitors. *PLOS ONE* **2016**, *11* (2), e0149659.
697 https://doi.org/10.1371/journal.pone.0149659.
698 (38) Jackson, P. A.; Widen, J. C.; Harki, D. A.; Brummond, K. M. Covalent Modifiers: A Chemical
699 Perspective on the Reactivity of α,β-Unsaturated Carbonyls with Thiols via Hetero-Michael
700 Addition Reactions. *J. Med. Chem.* **2017**, *60* (3), 839–885.
701 https://doi.org/10.1021/acs.jmedchem.6b00788.
702 (39) Singh, J.; Petter, R. C.; Baillie, T. A.; Whitty, A. The Resurgence of Covalent Drugs. *Nat. Rev.*
703 *Drug Discov.* **2011**, *10* (4), 307–317. https://doi.org/10.1038/nrd3410.
704 (40) Bauer, R. A. Covalent Inhibitors in Drug Discovery: From Accidental Discoveries to Avoided
705 Liabilities and Designed Therapies. *Drug Discov. Today* **2015**, *20* (9), 1061–1073.
706 https://doi.org/10.1016/j.drudis.2015.05.005.
707 (41) Potashman, M. H.; Duggan, M. E. Covalent Modifiers: An Orthogonal Approach to Drug Design.
708 *J. Med. Chem.* **2009**, *52* (5), 1231–1246. https://doi.org/10.1021/jm8008597.
709 (42) Labro, M. T. Anti-Inflammatory Activity of Macrolides: A New Therapeutic Potential? *J.*
710 *Antimicrob. Chemother.* **1998**, *41* (suppl_2), 37–46. https://doi.org/10.1093/jac/41.suppl_2.37.
711 (43) Krishnan, S.; Miller, R. M.; Tian, B.; Mullins, R. D.; Jacobson, M. P.; Taunton, J. Design of
712 Reversible, Cysteine-Targeted Michael Acceptors Guided by Kinetic and Computational Analysis.
713 *J. Am. Chem. Soc.* **2014**, *136* (36), 12624–12630. https://doi.org/10.1021/ja505194w.
714 (44) Serafimova, I. M.; Pufall, M. A.; Krishnan, S.; Duda, K.; Cohen, M. S.; Maglathlin, R. L.;
715 McFarland, J. M.; Miller, R. M.; Frödin, M.; Taunton, J. Reversible Targeting of Noncatalytic
716 Cysteines with Chemically Tuned Electrophiles. *Nat. Chem. Biol.* **2012**, *8* (5), 471–476.
717 https://doi.org/10.1038/nchembio.925.
718 (45) White, D. E.; Burchill, S. A. BAY 11-7082 Induces Cell Death through NF-KB-Independent
719 Mechanisms in the Ewing's Sarcoma Family of Tumours. *Cancer Lett.* **2008**, *268* (2), 212–224.
720 https://doi.org/10.1016/j.canlet.2008.03.045.
721 (46) García, M. G.; Alaniz, L.; Lopes, E. C.; Blanco, G.; Hajos, S. E.; Alvarez, E. Inhibition of NF-KB
722 Activity by BAY 11-7082 Increases Apoptosis in Multidrug Resistant Leukemic T-Cell Lines.
723 *Leuk. Res.* **2005**, *29* (12), 1425–1434. https://doi.org/10.1016/j.leukres.2005.05.004.
724 (47) Kolati, S. R.; Kasala, E. R.; Bodduluru, L. N.; Mahareddy, J. R.; Uppulapu, S. K.; Gogoi, R.;
725 Barua, C. C.; Lahkar, M. BAY 11-7082 Ameliorates Diabetic Nephropathy by Attenuating
726 Hyperglycemia-Mediated Oxidative Stress and Renal Inflammation via NF-KB Pathway. *Environ.*
727 *Toxicol. Pharmacol.* **2015**, *39* (2), 690–699. https://doi.org/10.1016/j.etap.2015.01.019.

728 (48) Goffi, F.; Boroni, F.; Benarese, M.; Sarnico, I.; Benetti, A.; Spano, P. F.; Pizzi, M. The Inhibitor of
729 IkappaBalpha Phosphorylation BAY 11-7082 Prevents NMDA Neurotoxicity in Mouse
730 Hippocampal Slices. *Neurosci. Lett.* **2005**, *377* (3), 147–151.
731 https://doi.org/10.1016/j.neulet.2004.11.088.
732 (49) Maier, L.; Pruteanu, M.; Kuhn, M.; Zeller, G.; Telzerow, A.; Anderson, E. E.; Brochado, A. R.;
733 Fernandez, K. C.; Dose, H.; Mori, H.; Patil, K. R.; Bork, P.; Typas, A. Extensive Impact of Non-
734 Antibiotic Drugs on Human Gut Bacteria. *Nature* **2018**, *555* (7698), 623–628.
735 https://doi.org/10.1038/nature25979.
736 (50) Cavallari, J. F.; Lamers, R. P.; Scheurwater, E. M.; Matos, A. L.; Burrows, L. L. Changes to Its
737 Peptidoglycan-Remodeling Enzyme Repertoire Modulate β-Lactam Resistance in *Pseudomonas*
738 *aeruginosa*. *Antimicrob. Agents Chemother.* **2013**, *57* (7), 3078–3084.
739 https://doi.org/10.1128/AAC.00268-13.
740 (51) Nguyen, U. T.; Wenderska, I. B.; Chong, M. A.; Koteva, K.; Wright, G. D.; Burrows, L. L. Small-
741 Molecule Modulators of *Listeria monocytogenes* Biofilm Development. *Appl. Environ. Microbiol.*
742 **2012**, *78* (5), 1454–1465. https://doi.org/10.1128/AEM.07227-11.
743 (52) Kunst, F.; Ogasawara, N.; Moszer, I.; Albertini, A. M.; Alloni, G.; Azevedo, V.; Bertero, M. G.;
744 Bessières, P.; Bolotin, A.; Borchert, S.; Borriss, R.; Boursier, L.; Brans, A.; Braun, M.; Brignell, S.
745 C.; Bron, S.; Brouillet, S.; Bruschi, C. V.; Caldwell, B.; Capuano, V.; Carter, N. M.; Choi, S.-K.;
746 Codani, J.-J.; Connerton, I. F.; Cummings, N. J.; Daniel, R. A.; Denizot, F.; Devine, K. M.;
747 Düsterhöft, A.; Ehrlich, S. D.; Emmerson, P. T.; Entian, K. D.; Errington, J.; Fabret, C.; Ferrari,
748 E.; Foulger, D.; Fritz, C.; Fujita, M.; Fujita, Y.; Fuma, S.; Galizzi, A.; Galleron, N.; Ghim, S.-Y.;
749 Glaser, P.; Goffeau, A.; Golightly, E. J.; Grandi, G.; Guiseppi, G.; Guy, B. J.; Haga, K.; Haiech, J.;
750 Harwood, C. R.; Hénaut, A.; Hilbert, H.; Holsappel, S.; Hosono, S.; Hullo, M.-F.; Itaya, M.; Jones,
751 L.; Joris, B.; Karamata, D.; Kasahara, Y.; Klaerr-Blanchard, M.; Klein, C.; Kobayashi, Y.; Koetter,
752 P.; Koningstein, G.; Krogh, S.; Kumano, M.; Kurita, K.; Lapidus, A.; Lardinois, S.; Lauber, J.;
753 Lazarevic, V.; Lee, S.-M.; Levine, A.; Liu, H.; Masuda, S.; Mauël, C.; Médigue, C.; Medina, N.;
754 Mellado, R. P.; Mizuno, M.; Moestl, D.; Nakai, S.; Noback, M.; Noone, D.; O'Reilly, M.; Ogawa,
755 K.; Ogiwara, A.; Oudega, B.; Park, S.-H.; Parro, V.; Pohl, T. M.; Portetelle, D.; Porwollik, S.;
756 Prescott, A. M.; Presecan, E.; Pujic, P.; Purnelle, B.; Rapoport, G.; Rey, M.; Reynolds, S.; Rieger,
757 M.; Rivolta, C.; Rocha, E.; Roche, B.; Rose, M.; Sadaie, Y.; Sato, T.; Scanlan, E.; Schleich, S.;
758 Schroeter, R.; Scoffone, F.; Sekiguchi, J.; Sekowska, A.; Seror, S. J.; Serror, P.; Shin, B.-S.; Soldo,
759 B.; Sorokin, A.; Tacconi, E.; Takagi, T.; Takahashi, H.; Takemaru, K.; Takeuchi, M.; Tamakoshi,
760 A.; Tanaka, T.; Terpstra, P.; Tognoni, A.; Tosato, V.; Uchiyama, S.; Vandenbol, M.; Vannier, F.;
761 Vassarotti, A.; Viari, A.; Wambutt, R.; Wedler, E.; Wedler, H.; Weitzenegger, T.; Winters, P.;

762 Wipat, A.; Yamamoto, H.; Yamane, K.; Yasumoto, K.; Yata, K.; Yoshida, K.; Yoshikawa, H.-F.;
763 Zumstein, E.; Yoshikawa, H.; Danchin, A. The Complete Genome Sequence of the Gram-Positive
764 Bacterium *Bacillus subtilis*. *Nature* **1997**, *390* (6657), 249–256. https://doi.org/10.1038/36786.
765 (53) Yao, Z.; Valvano, M. A. Genetic Analysis of the O-Specific Lipopolysaccharide Biosynthesis
766 Region (Rfb) of *Escherichia coli* K-12 W3110: Identification of Genes That Confer Group 6
767 Specificity to Shigella Flexneri Serotypes Y and 4a. *J. Bacteriol.* **1994**, *176* (13), 4133–4143.
768 https://doi.org/10.1128/jb.176.13.4133-4143.1994.
769 (54) Snitkin, E. S.; Zelazny, A. M.; Thomas, P. J.; Stock, F.; Program, N. C. S.; Henderson, D. K.;
770 Palmore, T. N.; Segre, J. A. Tracking a Hospital Outbreak of Carbapenem-Resistant *Klebsiella*
771 *pneumoniae* with Whole-Genome Sequencing. *Sci. Transl. Med.* **2012**, *4* (148), 148ra116-
772 148ra116. https://doi.org/10.1126/scitranslmed.3004129.
773 (55) Farha, M. A.; Verschoor, C. P.; Bowdish, D.; Brown, E. D. Collapsing the Proton Motive Force to
774 Identify Synergistic Combinations against *Staphylococcus aureus*. *Chem. Biol.* **2013**, *20* (9),
775 1168–1178. https://doi.org/10.1016/j.chembiol.2013.07.006.
776 (56) Epand, R. F.; Pollard, J. E.; Wright, J. O.; Savage, P. B.; Epand, R. M. Depolarization, Bacterial
777 Membrane Composition, and the Antimicrobial Action of Ceragenins. *Antimicrob. Agents*
778 *Chemother.* **2010**, *54* (9), 3708–3713. https://doi.org/10.1128/AAC.00380-10.
779 (57) Henriksbo, B. D.; Lau, T. C.; Cavallari, J. F.; Denou, E.; Chi, W.; Lally, J. S.; Crane, J. D.;
780 Duggan, B. M.; Foley, K. P.; Fullerton, M. D.; Tarnopolsky, M. A.; Steinberg, G. R.; Schertzer, J.
781 D. Fluvastatin Causes NLRP3 Inflammasome-Mediated Adipose Insulin Resistance. *Diabetes*
782 **2014**, *63* (11), 3742–3747. https://doi.org/10.2337/db13-1398.
783 (58) Henriksbo, B. D.; Tamrakar, A. K.; Xu, J.; Duggan, B. M.; Cavallari, J. F.; Phulka, J.; Stampfli,
784 M. R.; Ashkar, A. A.; Schertzer, J. D. Statins Promote Interleukin-1β–Dependent Adipocyte
785 Insulin Resistance Through Lower Prenylation, Not Cholesterol. *Diabetes* **2019**, *68* (7), 1441–
786 1448. https://doi.org/10.2337/db18-0999.
787
788
789
790
791
792
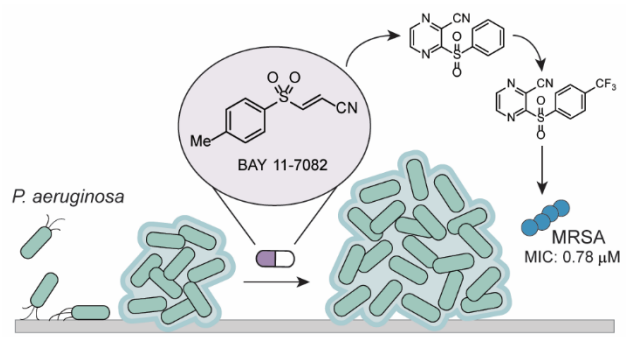
For Table of Contents only: